Biosensors and Bioelectronics 26 (2011) 3812–3817

Contents lists available at ScienceDirect

Biosensors and Bioelectronics

journal homepage: www.elsevier.com/locate/bios

Electrochemical biosensor based on nanoporous gold electrode for detection of PML/RARα fusion gene

Guangxian Zhong[a,1], Ailin Liu[a,b,1], Xuhai Chen[c,f], Kun Wang[d], Zhixian Lian[a], Qicai Liu[e], Yuanzhong Chen[a,b,*], Min Du[c,**], Xinhua Lin[a,***]

[a] Department of Pharmaceutical Analysis, Faculty of Pharmacy, Fujian Medical University, Fuzhou 350004, China
[b] Fujian Institute of Hematology, The Affiliated Union Hospital of Fujian Medical University, Fuzhou 350000, China
[c] Fujian Key Lab of Medical Instrumentation and Pharmaceutical Technology, Fuzhou University, Fuzhou, Fujian 350002, China
[d] Department of Pharmacy, The First Affiliated Hospital of Xiamen University, Xiamen 361003, China
[e] Department of Clinical Laboratory, The First Affiliated Hospital of Fujian Medical University, Fuzhou 350004, China
[f] College of Electrical Engineering and Automation, Fuzhou University, Fuzhou 350000, China

ARTICLE INFO

Article history:
Received 11 December 2010
Received in revised form 20 February 2011
Accepted 22 February 2011
Available online 1 March 2011

Keywords:
Nanoporous gold electrode
Square-wave oxidation reduction cycle
DNA biosensors
PML/RARα fusion gene
Methylene Blue

ABSTRACT

In this study, a kind of nanoporous gold electrode (NPG) prepared with repetitive square-wave oxidation reduction cycle (SWORC) was reported. The active surface area of the proposed NPG electrode was 9.9 times larger than that of a bare flat one characterized by cyclic voltammetry (CV). An electrochemical DNA biosensor based on NPG electrode was fabricated for detection of promyelocytic leukemia/retinoic acid receptor α (PML/RARα) fusion gene in acute promyelocytic leukemia (APL) by using Methylene Blue (MB) as an electroactive indicator. Differential pulse voltammetry (DPV) was employed to monitor the hybridization reaction on the probe modified electrode. The decrease of the peak current of MB was observed upon hybridization of the probe with target DNA. The results indicated that the peak current was linear with the concentration of complementary strand in the range of 60 pM to 220 pM with a detection limit of 6.7 pM. This new biosensor exhibited excellent sensitivity and selectivity and had been used for an assay of PCR real sample with a satisfactory result.

1. Introduction

Electrochemical DNA biosensor, as a monitoring technique, is widely considered to be a promising way for diagnosis of genetic diseases and other biological analysis due to their rapid and sensitive response as well as the simple and convenient operation (Bagni et al., 2006; Lee et al., 2008; Liu et al., 2008). The introduction of nanomaterials and nanotechnologies has greatly improved the sensitivity and selectivity of electrochemical DNA biosensors (Hahm and Lieber, 2004). In recent years, high-surface-area nanoporous gold (NPG) has attracted increasing attention due to its fascinating properties such as superior conductivity, large surface area, high stability and biocompatibility. Several methods such as electrochemical deposition (Shin et al., 2003; Li et al., 2011), a liquid-crystal template technique (Luo et al., 2004), organic templating (Walsh et al., 2003; Zhang et al., 2004), "direct freezing" (Zhang et al., 2005), a voltage-induced dimension change method (Weissmuller et al., 2003), "dealloying process" (Jia et al., 2007) and repetitive square-wave oxidation reduction cycle (SWORC) (Gamero et al., 2010) were reported to prepare nanoporous gold. Among these methods, SWORC is very attractive due to its easy, time-saving and controllable preparation for nanoporous gold.

SWORC is an important method for the surface pretreatment which can easily and quickly obtain the roughening surface. Bilmes et al. (1989) reported the application of SWORC in the formation of roughened platinum electrode which was used for the enhancement of surface-enhanced Raman scattering (SERS). Cai et al. (1998) prepared roughened platinum electrode with different roughness factors by using repetitive SWORC and investigated the influences of roughening pretreatment on surface Raman signals, enhancement factors and surface homogeneity at roughened Pt electrode. Recently, Gamero et al. (2010) developed a biosensor for the detec-

* Corresponding author at: Fujian Institute of Hematology, the Affiliated Union Hospital of Fujian Medical University, Fuzhou 350000, China.
Tel.: +86 591 83351966; fax: +86 591 83324116.
** Corresponding author at: Fujian Key Lab of Medical Instrumentation and Pharmaceutical Technology, Fuzhou University, Fuzhou, Fujian, 350002, China.
Tel.: +86 591 83759450; fax: +86 591 83759450.
*** Corresponding author at: Department of Pharmaceutical Analysis, Faculty of Pharmacy, Fujian Medical University, Fuzhou 350004, China.
Tel.: +86 591 22862016; fax: +86 591 22862016.
E-mail addresses: chenyz@pub3.fz.fj.cn (Y. Chen), mingdu@fzu.edu.cn (M. Du), xhl1963@sina.com (X. Lin).
[1] These authors contributed equally to the present study.

0956-5663/$ – see front matter © 2011 Elsevier B.V. All rights reserved.
doi:10.1016/j.bios.2011.02.039

tion of lactate using a nanostructured rough gold surface prepared with repetitive SWORC as transducer.

Acute promyelocytic leukemia (APL) is a clonal expansion of hematopoietic precursors blocked at the promyelocytic stage (Raymond et al., 1993). APL is characterized by a 15;17 chromosome translocation with breakpoints within the retinoic acid alpha receptor α (RARα) gene on chromosome 17 and the promyelocytic leukemia (PML) gene, which encodes a putative transcription factor, on chromosome 15. The translocation creates a PML/RARα fusion gene which produces a chimeric protein. This fusion protein binds with enhanced affinity to sites on the cell's DNA, blocking transcription and differentiation of granulocytes (Goddard et al., 1991; de The et al., 1990; Pandolfi et al., 1991; Wang et al., 2011). Thus, the PML/RARα fusion gene is a biomarker of APL, and is also a gold standard in clinical diagnosis. The PML/RARα fusion gene has become diagnostic for APL, as it is present in almost 100% of cases (Borrow et al., 1990; Wei et al., 2009). Early diagnosis of this disease is essential because of the associated life-threatening coagulopathy and the unique response of the disease to all-trans retinoic acid (ATRA) therapy. The detection of this PML/RARα fusion gene will afford an early diagnosis and monitor of APL. The reported monitoring methods of clinical diagnosis and prognosis about PML/RARα fusion gene included chromosome analysis (Yoo et al., 2006), fluorescence in situ hybridization (FISH) (Amare et al., 2001), flow cytometry (FCM) (Tirado et al., 2003), real-time quantitative reverse transcription polymerase chain reaction (RT-PCR) (Han et al., 2007), etc. But there were some limitations in these methods, such as time consuming, poor precision, and expensiveness. Thus, it was very significant to develop a new effective method to detect the PML/RARα fusion gene.

In the present work, an electrochemical DNA biosensor based on the nanoporous gold electrode prepared with repetitive SWORC was fabricated for the detection of PML/RARα fusion gene existed in APL. The nanoporous gold electrode was first covalently assembled with the probe DNA, followed by the hybridization with the PML/RARα fusion gene in APL. DPV was employed to monitor the variation of pre and post hybridization by using MB as electroactive indicator. This new pattern showed excellent sensitivity and specificity and had been used for assay of the PCR real sample with a satisfactory result.

2. Materials and methods

2.1. Materials and chemicals

All synthetic oligonucleotides designed according to the PML/RARα fusion gene were purchased from TaKaRa Biotechnology (Dalian, China) Co., Ltd. Their base sequences were as follows: immobilized probe (22-base sequence S1)-5′-SH-GGT CTC AAT GGC TGC CTC CCC G-3′; target DNA (22-base sequence S2)-5′-CGG GGA GGC AGC CAT TGA GAC C-3′; single-mismatched DNA (22-base sequence S3)-5′-CGG GGA GGC ACC CAT TGA GAC C-3′; partial PML (22-base sequence S4)-5′-CGG GGA GGC AGA GGA ACG CGT T-3′; partial RARα (22-base sequence S5)-5′-ATC CCC AGC CAC CAT TGA GAC C-3′. Ethylenediamine-tetraacetic acid (EDTA) and mercaptohexanol (MCH) were purchased from Sigma–Aldrich (St. Louis, MO, USA). Tris (2-carboxyethyl) phosphine hydrochloride (TCEP) was purchased from Shanghai Sangon Biological Engineering Technology Services Reagents Co., Ltd. (China). Methylene Blue (MB) was purchased from Aldrich. All other chemicals were of analytical grade.

Stock solutions of MB (1.0 mM) were prepared with deionized water. The buffers involved in this work were as follows: DNA immobilization buffer, 10 mM Tris–HCl, 1.0 mM EDTA, 10 mM TCEP (pH 7.4) and 1.0 M NaCl; hybridization buffer was 1 M NaCl and 10 mM PBS buffer (pH 7.4); washing buffer was 0.1 M NaCl and 10 mM PBS buffer (pH 7.4). All solutions were prepared with deionized water (18.2 MΩ cm resistivity) from a Millipore system.

2.2. Apparatus

Electrochemical measurements were performed on a CHI 760D Electrochemical Workstation (CH Instrument, USA) using a traditional three-electrode system. The nanoporous gold electrode was used as working electrode, a platinum wire and Ag/AgCl electrode were used as counter electrode and reference electrode, respectively. All potentials herein were referred to this reference electrode. Differential pulse voltammetry (DPV) was carried out from −0.40 to 0.00 V with an amplitude of 50 mV. SEM images were obtained from XL-30E scanning electron microscopy (Philips, The Netherlands).

2.3. Fabrication of nanoporous gold electrode

A schematic representation of the novel sensor fabrication procedure was illustrated in Scheme 1. A gold electrode (2 mm in diameter) was polished before each experiment with 1.0, 0.3 and 0.05 μm alumina powder, respectively, and sonicated in ethanol and deionized water thoroughly. After electrochemically cleaning in fresh 0.5 M H_2SO_4 solution to remove any possible impurities on the surface (Fan et al., 2003), the gold electrode was then subjected to a repetitive SWORC procedure for its surface to be roughened. The procedure was carried out in two consecutive stages as follows: Firstly, a relatively thick hydrous gold oxide layer was accumulated on the gold electrode immersed in 0.5 M sulphuric acid by using repetitive square wave potential between −0.8 V and 2.5 V (versus Ag/AgCl electrode) at 2000 Hz for a time of 5 min. Subsequently, the potential was held at −0.8 V until the complete electroreduction of the hydrous gold oxide layer was accomplished (Bilmes et al., 1989), then the resulting nanoporous gold electrode was sonicated in deionized water for 1 min and cycled at 0.1 V/s between −0.35 and 1.5 V in 0.5 M H_2SO_4 solution to clean the surface of the electrode, and check variations in the electroadsorption charge of the O adatoms between the rough Au electrode and flat Au electrode.

2.4. Preparation of DNA biosensor based on NPG electrode

The cleaned NPG electrode was used for the preparation of the DNA biosensor by incubation in an immobilization buffer containing 10 μM capture probe modified with thiolate for 2 h at room

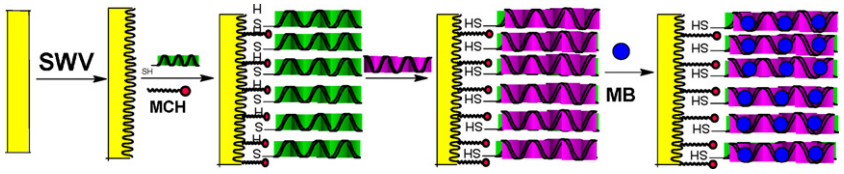

Scheme 1. Schematic representation of the fabrication procedure of DNA biosensor based on NPG-electrode.

temperature. The single-stranded DNA (ssDNA) modified electrode was then treated with 1.0 mM MCH for 1 h to obtain a well-aligned ssDNA/MCH modified electrode, followed by thoroughly washing with deionized water to remove unspecific adsorbed DNA probe. For the hybridization reaction, the ssDNA/NPG electrode was immersed in PBS solution containing synthetic targets or PCR real samples for 30 min at 45 °C (Lin et al., 2007). The PCR real samples should be heated at 95 °C for 10 min and cooled in ice bath before use. After that, the hybrid-modified NPG electrode was washed with deionized water and immersed in 0.1% SDS phosphate buffer (pH 7.40) to remove unbound oligonucleotides before MB accumulation.

2.5. MB accumulation and voltammetric transduction

MB is an organic dye and an electron transfer mediator which interacts in different ways with ssDNA and double-stranded DNA (dsDNA) (Kerman et al., 2002). The voltammetric reduction signals of MB reflect the extent of the hybrid formation. MB was accumulated onto hybrid-modified NPG electrode by immersing the electrode into the stirring 10 mM PBS buffer solution (pH 7.4) containing 20 μM MB for 10 min without applying any potential (Lin et al., 2007). After accumulation of MB, the electrode was rinsed with watching buffer in an ultrasonic bath for 10 s to remove the non-specifically bound MB. MB was intercalated into the DNA to form a DNA/MB system on the probe modified electrode. Subsequently, the electrode was transferred into the 10 mM PBS buffer solution and scanned from −0.40 to 0.00 V with an amplitude of 50 mV by using DPV.

3. Results and discussion

3.1. Characterization of the nanoporous gold electrode

Fig. 1A showed the SEM images of the gold surface morphology before and after the pretreatment of repetitive SWORC. SEM images of the rough gold electrode revealed the presence of small grains and channels of about 120 nm in width. The brain-like aspect showed in SEM images had been reported previously as characteristic of the gold overlayers resulting from electroreduction process (Vazquez et al., 1989). In fact, the more important characteristic features were the voids not the grains. Since the roughness was determined by the average area of three dimensional electrodeposit formed by a rectangular array of columns of average height h and average radii r terminated with a hemispherical dome of the same radius, of C_{4v} symmetry, it was possible to estimate these parameters from electrochemical data (Gamero et al., 2010; Vazquez et al., 1989).

The NPG electrode was electrochemically characterized in a solution of 0.5 M H_2SO_4 at a scan rate of 100 mV/s (Fig. 1B, curve (b)). For comparison, the cyclic voltammogram (CV) of a bare flat gold electrode with the same geometric surface area under the same condition was also presented in Fig. 1B, curve (a). The CV curve of nanoporous gold electrode appeared three oxidation current peaks for the formation of gold oxide at potentials positive to 1.05 V and a reduction peak in the reversed potential sweep due to the reduction of gold oxides. By integrating the charge required for reducing the gold oxide formed in the positive sweep, the real surface of NPG electrode was determined to be 1.01 cm^2 by assuming that the reduction of monolayer of gold oxide requires 386 $\mu C\,cm^{-2}$ (Gao et al., 2007), and the roughness factor was about 32, which was approximately 9.9 times larger than that of a flat gold electrode with the same geometric area. Obviously, the NPG electrode had a much larger real surface area than that of a flat electrode with the same geometric area.

3.2. Characterization of the biosensor based on nanoporous gold electrode

In order to confirm the preparing process of NPG-based biosensor, electrochemical impedance spectroscopy (EIS) was employed to monitor the changes of each step in the construction of

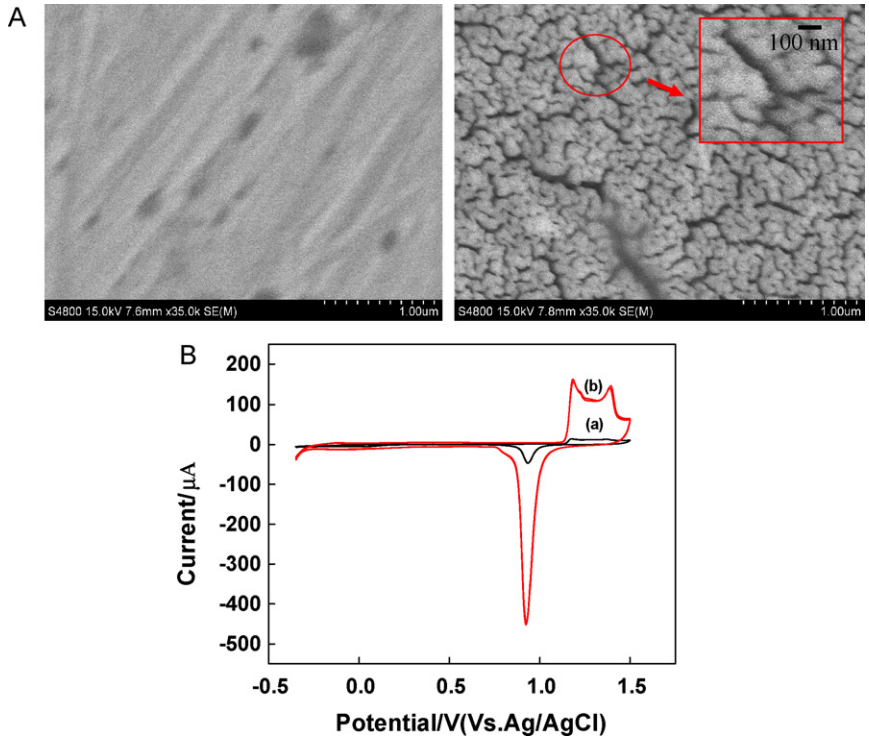

Fig. 1. (A) SEM images of the same gold electrode before and after the pretreatment of SWORC. (B) Cyclic voltammograms (CV) of a nanoporous gold electrode (curve (b)) and a flat gold electrode (curve (a)) with the same geometric area in a solution of 0.5 M H_2SO_4 at a scan rate of 100 mV/s.

biosensor. The EIS experiments were performed in a solution of 0.1 M KCl containing 10 mM $K_3Fe(CN)_6$ + 10 mM $K_4Fe(CN)_6$ at a potential of 0.2 V(versus Ag/AgCl) in the frequency range of 0.05–10^5 Hz. The impedance spectra included a semicircle portion at higher frequencies corresponding to the electro-transfer-limited process and a linear portion at lower frequencies representing the diffusion-limited process. The semicircle diameter equalled the electro-transfer resistance, R_{et}. Fig. 2 showed the Faradaic impedance spectra observed upon the stepwise modification process with the NPG electrode (Fig. 2A) and bare flat gold electrode (Fig. 2B). The inset was the electrical equivalent circuit. The circuit, which is often used to model interfacial phenomenon, includes the following elements: (i) Rs, the ohmic resistance of electrolyte solution. (ii) R_{et}, the electro transfer resistance, which exists if redox probe is present in the electrolyte solution. (iii) CPE, a constant phase element simulating a non-ideal behaviour capacitor. (iv) Zw, the Warburg impedance, resulting from the diffusion of ions from the bulk electrolyte to the electrode interface. Ideally, Zw and Rs represent the bulk properties of the electrolyte solution and diffusion features of the redox probe in solution and, thus, are not affected by modifications on the electrode surface. As can be seen in Fig. 2A, the changes in R_{et} were much larger than those in other impedance components. Thus, R_{et} was a suitable signal for sensing the interfacial properties of the prepared biosensor during all these assembly procedures.

For the bare flat gold electrode, the value of R_{et} was 57.7 Ω, revealing a very small semicircle domain. When the probe was self-assembled onto the electrode surface, the value of R_{et} increased from 57.7 Ω to 5370 Ω due to the electrostatic repulsion between the negatively charged probe and the negatively charged redox probe $[Fe(CN)_6]^{3-/4-}$ (Cho et al., 2006). Subsequently, the target DNA was hybridized with probe to form the dsDNA, and the value of R_{et} increased to 8527 Ω due to large amount of negatively charged DNA linked on the electrode surface. For the NPG electrode, the value of R_{et} in each modification step decreased sharply compared with corresponding step for flat gold electrode, which indicated that the NPG electrode possessed high conductivity due to its nanoporous architecture.

3.3. Electrochemical response of MB-bound probe

The detection of hybridization was accomplished by using MB (Erdem et al., 2000), where reversible electroactivity and strong association with the immobilized probe led to significant enhanced voltammetric signals. It should be pointed out that MB interacted in two kinds of ways with ssDNA and dsDNA. According to the report by Kerman et al. (2002), the binding of MB with ssDNA and dsDNA resulted in variation in electrochemical response of MB on DNA modified electrode. The reduction signal of MB increased in the presence of probe at the NPG electrode surface due to the specific binding of MB with guanine bases. After hybridization with target DNA, the reduction signal decreased because the steric structure of dsDNA blocked the interaction of MB with guanine bases. Thus, the decrease in the magnitude of the voltammetric reduction signals of MB reflected the extent of hybrid formation. As shown in Fig. 3, curve (b) was the DPV of MB bound to ssDNA at flat gold electrode surface, curve (a) was the DPV of MB intercalated into corresponding dsDNA at flat gold surface. The peak current difference of these two curves was 1.046 μA, indicating that MB desorbed from dsDNA. Curve (d) corresponded to the reduction signal of ssDNA at NPG electrode surface, while curve (c) related to the reduction signal of corresponding dsDNA at NPG electrode surface, the difference

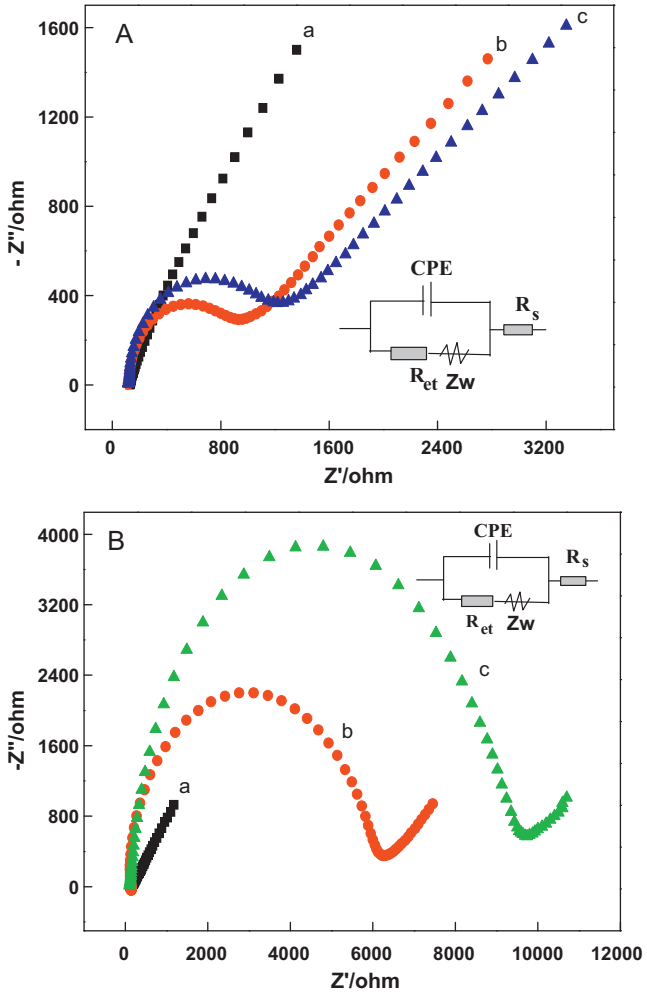

Fig. 2. Impedance spectra (Nyquist plots) corresponding to NPG electrode (A) and flat gold electrode (B). (a) The bare electrode, (b) after immobilization of capture probe, and (c) hybridization with target DNA. The data were recorded in the presence of 10 mM $[Fe(CN)_6]^{4-/3-}$ as redox label. The biased potential was 0.08 V (versus Ag/AgCl) in the frequency range of 0.05–10^5 Hz and the amplitude was 5.0 mV.

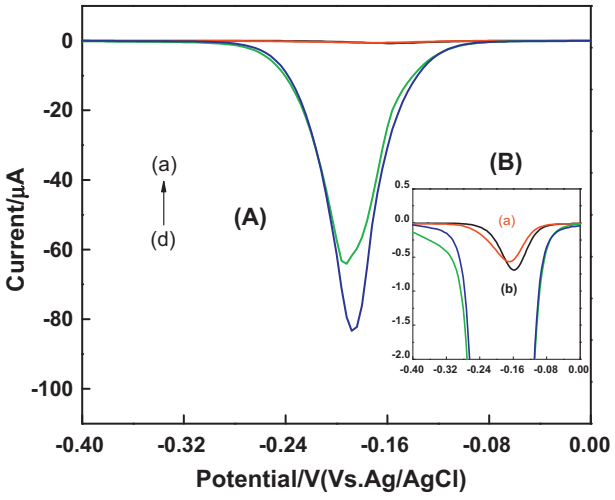

Fig. 3. Differential pulse voltammetry for 20 μM MB as redox indicator at a probe modified flat gold electrode (b) and after hybridization with the complementary target DNA (a), a probe modified nanoporous gold electrode (d) and after hybridization with the complementary DNA (c). The initial potential was 0.4 V; the final potential was −0.5 V, the amplitude was 0.05 V, the pulse width was 0.05 s; the pulse cycle was 0.2 s; the sample interval was 0.0167 V; and the standing time was 2 s. Buffer solution: 10 mM PBS (pH 7.4) containing 1 M NaCl.

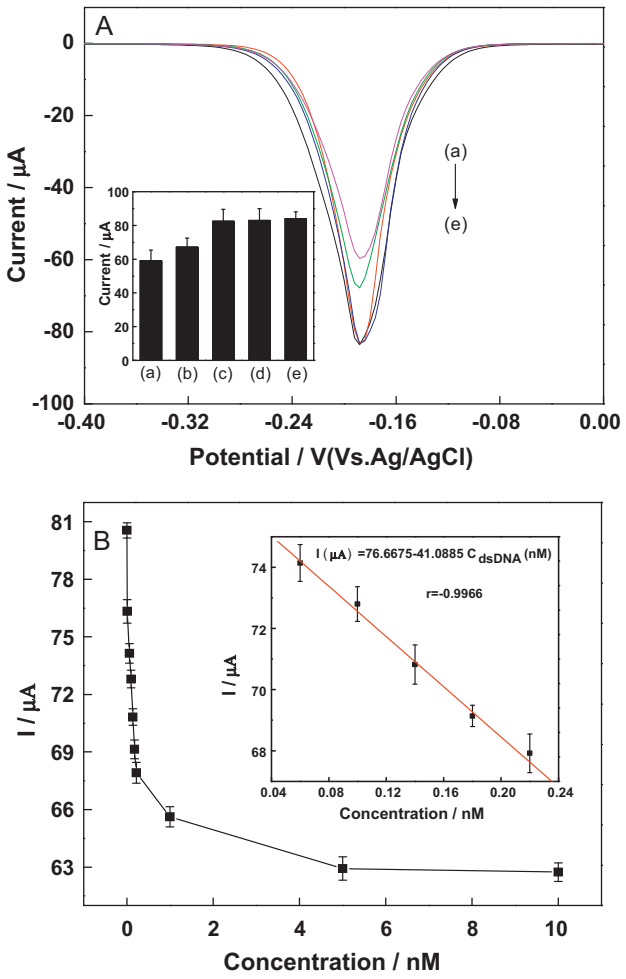

Fig. 4. (A) Differential pulse voltammetry using 20 μM MB as redox indicator for a probe modified flat gold electrode (e) and after hybridization with the complementary target sequence (a), one-base-mismatch sequence (b), PML sequence (c) and RARα sequence (d). The experimental conditions are as in this figure. (B) Response of the probe with increasing concentration of target oligonucleotides. The concentration of target DNA was observed in a range from 1 pM to 10 nM. Inset shows the plot of the peak current of MB as a function of the target concentration. The concentration of target DNA was 60 pM, 100 pM, 140 pM, 180 pM, 220 pM. Error bars, relative standard deviation of three independent experiments. Other experimental conditions are as in this figure.

of these two peak currents was 25.16 μA. Compared with flat gold electrode, the peak current difference of NPG electrode was about 25 times higher, which demonstrated that the NPG-based biosensor greatly increased the efficiency of hybridization.

3.4. Selectivity of the NPG-based biosensor

Detection of target DNA was also monitored by measuring the peak current of MB absorbed on the NPG electrode with DPV. The selectivity of this assay in discriminating complementary DNA (S2) from one base mismatched DNA (S3), partial PML (S4) and partial RARα (S5) was investigated as shown in Fig. 4A. It was clear that the highest peak current signal of MB was obtained on the ssDNA modified NPG electrode (Fig. 4A curve (e)). After hybridization with complementary DNA, the peak current of MB was decreased dramatically (Fig. 4A curve (a)), which indicated that probe had completely hybridized with complementary DNA. In the presence of single base mismatched DNA, the signal of MB (Fig. 4A curve (b)) was significantly increased compared with complementary DNA, demonstrating that the complete hybridization was not accomplished due to the base mismatch. Moreover, no significant difference of peak current could be observed for ssDNA and its hybridization with partial PML and partial RARα as expected. Fig. 4A curves (c and d), since no successful hybridization occurred due to the sequence mismatch between the probe and those partial complementary sequences.

3.5. Sensitivity of the NPG-based biosensor

The sensitivity of the NPG-based biosensor for complementary target DNA at different concentration was investigated according to the protocol mentioned in Section 2. The different peak current values of MB were collected by three repetitive measurements of hybridization of the probe with target DNA. The current response at about −0.19 V decreased in proportion to the amount of the target DNA used. Electrochemical responses of the target DNA with different concentration could also be quantitatively analyzed. The responses of the probe for increasing concentration levels of the target DNA were displayed in Fig. 4B. The peak current values decreased with the increase of the concentration of target DNA, ranging from 1.0 pM to 10 nM, and then the values tended to remain constant, indicating that all the available immobilized probe on the NPG electrode surface had involved in hybridization. The decrease of the reduction signal of MB was due to the formation of duplex which blocked the interaction of MB with guanine base. Inset showed that the linear range was from 60 pM to 220 pM, with the regression equation being $I\,(\mu A) = -41.0885 C_{dsDNA}\,(nM) + 76.6675$, $R = -0.9966$. A detection limit of 6.7 pM target DNA could be estimated using 3σ (where σ is the standard deviation of the blank solution, $n = 8$). The reproducibility of the biosensor for detection of 0.12 nM target DNA was 7.26% ($n = 3$).

3.6. Detection of PCR products

All the PCR samples were obtained from Fujian Institute of Hematology. The positive real sample contained a PCR product that had a sequence complementary to the specific PML/RARα probe, while the PCR product from a negative real sample contained a sequence noncomplementary to the specific PML/RARα probe. As the blank background, the PCR buffer system, which did not contain any DNA templates, was also studied.

Fig. 5A represented the DPV signals of MB obtained when the probe for PML/RARα was immobilized and different real samples were used in the hybridization step. The DPV signals of MB obtained from the probe-modified NPG-based biosensor gave a mean average of 75.9 μA with a RSD of 6.16%. The blank background was measured and the signals gave a mean average of 64.8 μA with a RSD of 6.89%. DPV signals of MB obtained from the hybridization of the probe with the positive and negative real samples gave a mean average of 57.6 μA with a RSD of 7.69% and 73.8 μA with a RSD of 8.35%, respectively. The MB signal from the probe modified NPG electrode (Fig. 5A curve (a)) was much higher than that of the probe modified NPG electrode after hybridization with a positive real sample (Fig. 5A curve (d)). The obvious decrease in the magnitude of the MB signal obtained with positive real samples was observed. The decrease of DPV signals showed that hybridization at NPG electrode surface was occurred and MB could not interact with the bound guanine bases of the hybrid. The decrease in the reduction of MB was attributed to the steric inhibition of the reducible groups of the intercalated MB because of the formation of hybrid at the NPG electrode surface. If the blood sample was a negative real sample, the amplified PCR product would not contain a target sequence complementary to the specific probe. Thus, the interaction between these negative real samples and the immobilized probes did not lead to hybridization and the magnitude of the

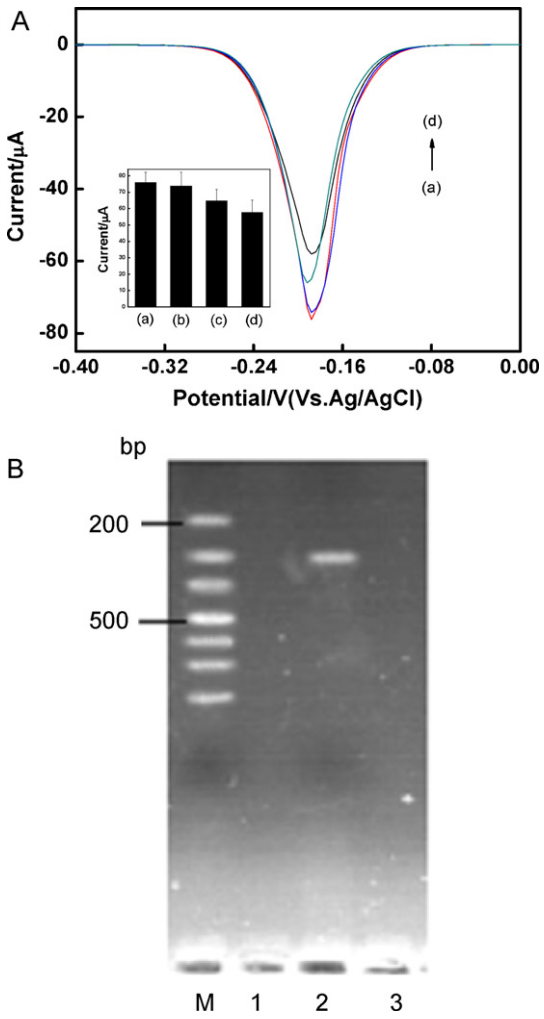

Fig. 5. (A) Differential pulse voltammetry using 20 μM MB as redox indicator for a probe modified flat gold electrode (a), the blank background (c), after hybridization with the positive sample (d) and negative sample (b). Error bars, relative standard deviation of three independent experiments. The experimental conditions are as in Fig. 4. (B) The electropherogram of PCR products. The lanes from left to right: (1) negative real sample, (2) positive real sample and (3) blank background.

MB signal was nearly as high as the probe signal (Fig. 5A curves (a and b)). Additionally, the PCR real samples were also characterized with 1.5% agarose gel electrophoresis as described by literature methods (Akarca et al., 1994). Fig. 5B showed the electropherogram of PCR products. The PCR amplification products from positive real samples (Fig. 5B, lane 2) showed the light brands in the 1.5% agarose gel. However, the PCR products from negative real samples (Fig. 5B, lane 1) and blank background (Fig. 5B, lane 3) did not present any light brands in the gel. The results obtained from the electrochemical DNA biosensor were in good agreement with the ones obtained from gel electrophoresis.

4. Conclusion

An electrochemical biosensor based on NPG electrode was fabricated and exhibited excellent sensitivity and selectivity for detection of PML/RARα fusion gene. The fabrication of NPG electrode was quite simple, economical and controllable, which were main advantages of the present biosensor. The relatively high selectivity and sensitivity could be attributed to the NPG electrode with superior conductivity, high surface area and biocompatibility. This new biosensor had been used for assay of the complementary sequence in the PCR amplified real samples with satisfactory results. While the concept in this study has been demonstrated in connection with PCR real samples for the detection of APL, further improvements may be achieved to detect quantitative target sequences from real samples directly, and solve the actual problem of the early diagnosis and prognosis monitor of APL and other diseases.

Acknowledgements

The authors gratefully acknowledge the financial support of the National High Technology and Development of China (863 Project: 2008AA02Z433), the National Natural Science Foundation of China (20805006 and 20975021), the Fujian Provincial University-Industry Cooperation Science & Technology Major Program (2010Y4003), the Foundation of Fujian Key Laboratory of Hematology (2009J1004), the Scientific Research Major Program of Fujian Medical University (09ZD013), and the Natural Science Foundation of Fujian Province of China (2010J06011) and Excellent Youth Talent Program of the Fujian Province University (JA10126).

References

Akarca, U.S., Greene, S., Lok, A., 1994. Hepatology 19, 1366–1370.
Amare, P.S., Baisane, C., Saikia, T., Nair, R., Gawade, H., Advani, S., 2001. Cancer Genet. Cytogenet. 131, 125–134.
Bagni, G., Osella, D., Sturchio, E., Mascini, M., 2006. Anal. Chim. Acta 573, 81–89.
Bilmes, S.A., Rubim, J.C., Otto, A.J., 1989. Chem. Phys. Lett. 159, 89–96.
Borrow, J., Goddard, A.D., Sheer, D., Solomon, E., 1990. Science 249, 1577–1580.
Cai, W.B., Ren, B., Li, X.Q., Se, C.X., Liu, F.M., Cai, X.W., Tian, Z.Q., 1998. Surf. Sci. 406, 9–22.
Cho, M., Lee, S., Han, S.Y., Park, J.Y., Rahman, M.A., Shim, Y.B., Ban, C., 2006. Nucleic Acids Res. 34, e75.
de The, H., Chomienne, C., Lanotte, M., Degos, L., Dejean, A., 1990. Nature 347, 558–561.
Erdem, A., Kerman, K., Meric, B., Akarca, U.S., Ozsoz, M., 2000. Anal. Chim. Acta 422, 139–149.
Fan, C., Plaxco, K.W., Heeger, A.J., 2003. Proc. Natl. Acad. Sci. U.S.A. 100, 9134.
Gamero, M., Pariente, F., Lorenzo, E., Alonso, C., 2010. Biosens. Bioelectron. 25, 2038.
Gao, W., Xia, X.H., Xu, J.J., Chen, H.Y., 2007. J. Phys. Chem. C 111, 12213–12219.
Goddard, A.D., Borrow, J., Freemont, P.S., Solomon, E., 1991. Science 254, 1371–1374.
Hahm, J., Lieber, C.M., 2004. Nano. Lett. 4, 51–54.
Han, J.Y., Kim, K.E., Kim, K.H., Park, J.I., Kim, J.S., 2007. Leuk. Res. 31, 239–243.
Jia, F., Yu, C., Ai, Z., Zhang, L., 2007. Chem. Mater. 19, 3648–3653.
Kerman, K., Ozkan, D., Kara, P., Meric, B., Gooding, J.J., Ozsoz, M., 2002. Anal. Chim. Acta 462, 39–47.
Lee, S.J., Youn, B.S., Park, J.W., Niazi, J.H., Kim, Y.S., Gu, M.B., 2008. Anal. Chem. 80, 2867–2873.
Li, F., Han, X.P., Liu, S.F., 2011. Biosens. Bioelectron. 26, 2619–2625.
Lin, X.H., Wu, P., Chen, W., Zhang, Y.F., Xia, X.H., 2007. Talanta 72, 468–471.
Liu, B., Lu, L., Wang, M., Zi, Y., 2008. Electroanalysis 20, 2363–2369.
Luo, H., Sun, L., Lu, Y., Yan, Y., 2004. Langmuir 20, 10218–10222.
Pandolfi, P.P., Grignani, F., Alcalay, M., Mencarelli, A., Biondi, A., LoCoco, F., Grignani, F., Pelicci, P.G., 1991. Oncogene 6, 1285–1292.
Raymond, P.W., Hugues, D.T., Zhen-Yi, W., Laurent, D., 1993. N. Engl. J. Med. 329, 177–189.
Shin, H.C., Dong, J., Liu, M., 2003. Adv. Mater. 15, 1610–1614.
Tirado, C.A., Golembiewski-Ruiz, V., Horvatinovich, J., Moore, J.O., Buckley, P.J., Stenzel, T.T., Goodman, B.K., 2003. Cancer Genet. Cytogenet. 145, 31–37.
Vazquez, L., Bartolome, A., Baro, A.M., Alonso, C., Salvarezza, R.C., Arvia, A.J., 1989. Surf. Sci. 215, 171–189.
Walsh, D., Arcelli, L., Ikoma, T., Tanaka, J., Mann, S., 2003. Nat. Mater. 2, 386–390.
Wang, K., Sun, Z.L., Feng, M.J., Liu, A.L., Yang, S.Y., Chen, Y.Z., Lin, X.H., 2011. Biosens. Bioelectron. 26, 2870–2876.
Wei, N., Chen, J.H., Zhang, J., Wang, K., Xu, X.W., Lin, J.H., Li, G.W., Lin, X.H., Chen, Y.Z., 2009. Talanta 78, 1227–1234.
Weissmuller, J., Viswanath, R.N., Kramer, D., Zimmer, P., Wurschum, R., Gleiter, H., 2003. Science 300, 312.
Yoo, S.J., Seo, E.J., Lee, J.H., Seo, Y.H., Park, P.W., Ahn, J.Y., 2006. Cancer Genet. Cytogenet. 167, 168–171.
Zhang, H., Hussain, I., Brust, M., Butler, M.F., Rannard, S.P., Cooper, A.I., 2005. Nat. Mater. 4, 787–793.
Zhang, H., Hussain, I., Brust, M., Cooper, A.I., 2004. Adv. Mater. 16, 27–30.